

# Development of oxide scale microstructure on single-crystal SiC

L. U. OGBUJI

*Department of Materials Science and Engineering, University of Florida, Gainesville, Florida 32611, USA*

Microstructures of oxide scales on SiC single crystals, produced by oxidation at 1400°C for various lengths of time, were studied by light and transmission electron microscopy and by X-ray diffraction. At short oxidation times the oxide films were amorphous; at longer times they consisted of spherulitic cristobalite. The cristobalite is thought to grow by devitrification of the amorphous phase. No significant difference in oxide scale thickness or structures was found between commercial purity and semiconductor grade crystals.

## 1. Introduction

Until recently SiC was generally available only as technical grade granules produced usually by the Acheson process and occasionally as a Lely-type crystal [1]. Much of the work on SiC oxidation was conducted on such granules, with consequent complication of the interpretation of results: such materials behave neither quite as individual single crystals nor as polycrystalline samples in oxidation and the results obtained were strongly dependent on the sample used. The coarser granules, essentially single crystals [2], oxidized differently from the powdery specimens whose kinetics were found to be strongly influenced by the granule size [3, 4]. There were also contradictions concerning the polymorphic phase and the structural details of the oxide formed. Shuster and Gugel [2] provide a survey of these.

Single crystals of SiC grown under controlled conditions are now available and their oxidation is yielding interesting observations on, among other things, the disparate rates of oxygen adsorption on different crystallographic faces [5] and of oxidation on faces of different polarity [6]\*; the effect of phase and polytypic modifications on the oxidation behaviour [2]; the role of temperature and pressures on the active/passive nature of the oxidation [7]; and the transition of

the oxide scale from amorphous silica to cristobalite [2, 8]. Nevertheless the works cited, excepting those of [2, 8], dealt mainly with oxidation kinetics. Yet oxide scale microstructure can reveal useful information on, for instance, the diffusion process limiting oxidation [8] and phase changes during oxidation [2]. The latter acquires special importance in view of the claims that crystalline SiO<sub>2</sub> may be less passivating than the vitreous form [4, 9, 10].

The investigation reported here was aimed at the evolution of scale microstructure during SiC oxidation in air. Single crystals were used for two main reasons: (1) their oxidation would be uncomplicated by substrate microstructure and phase content; (2) they are available in the relatively pure form (or with known impurity content): purity is usually a matter of considerable concern in SiC.

## 2. Experimental procedure

### 2.1. Material

Four different specimens were used. The first was technical grade SiC in the form of an intergrown mass of black single crystals, each exposing at least one well-developed basal face. This specimen came from Elektroschmelzwerke, Munich. The other specimens were of semiconductor purity and

\*Single-crystal SiC is plate-like in habit, being thinnest along the *c*-axis. The crystals are bounded along this axis by a plane of carbon atoms and an opposite plane of silicon atoms.

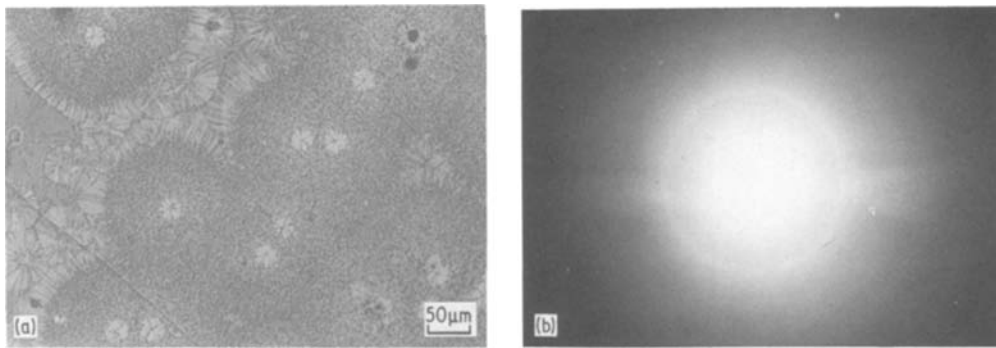


Figure 1 (a) Light micrograph and (b) electron diffraction pattern from oxide on a semiconductor grade SiC single crystal oxidized for 30 min at 1400° C. Strings of nascent spherulites occur, but the scale is still mostly amorphous (b).

in the form of transparent wafers, each bounded by two, well-developed basal surfaces. They differed only in their dopants and consequent colouration: a clear, undoped specimen, a green, N-doped specimen and a black, Al-doped specimen. The exact dopant levels were not determined, but are thought to lie well within the solubility limits of those elements in SiC at 2700° C, where the crystals were grown. The dopants could not be detected in the crystals by Auger Electron Spectroscopy or in the oxide scale by infra-red reflection spectroscopy. The supplier, R. Potter of General Electric (GE) Company, Nela Park, Cleveland, Ohio, specified the dopant in each case.

All four specimens were of the  $\alpha$ -phase, with 6H, 15R and 4H determined as the predominant polytypes, in that order.

## 2.2. Sample preparation and examination

The as-grown faces of the semiconductor grade specimens were optically smooth. The faces of the technical grade specimen, on the other hand, were unsuitable as-grown, containing inclusions, facets and defects; samples from this specimen were cut from the bulk. Sectioning was in every case parallel to the habit, (0001) faces. Transmission electron microscopy (TEM) sections were polished on both faces. Polishing was accomplished using diamond pastes in a sequence down to 1.0  $\mu\text{m}$ .

Samples were ultrasonically cleaned in alcohol and in dilute HF, placed on high-purity (99.9%) alumina boats (leaning at a corner) and oxidized in air at 1400° C.\* The oxide scales were examined at 0.5 h intervals up to 3 h, then at hourly intervals up to 6 h and finally at 3 h or 6 h intervals.

\*Oxidation times at 1300° C were inconveniently long; however, resultant oxide scale microstructures were similar to those presented here. At 1500° C oxidation was too rapid, and the early-stage microstructure reported here was not observed. Hence, unless otherwise stated, the oxide scales shown here were grown at 1400° C.

Oxidized TEM sections were mounted on slotted nickel discs or grids and ion-thinned from one side to preserve the oxide scale on the other side. Some oxidized coupons were sectioned normal to the oxide scale, mounted in epoxy, polished and etched in weak HF solution for the measurement of scale thickness.

Light microscopy was carried out using a Reichert metallograph with white light incident on the sample surface (in reflection mode). For TEM a Siemens 102 microscope was used, at 125 kV.

## 3. Results and discussion

### 3.1. Evolution of microstructure

Initial oxide films were amorphous. In most cases this was determined by electron diffraction, the films being too thin for X-ray detection in samples oxidized for less than about 1 h. Fig. 1a shows an oxide film grown for 0.5 h. While it has skeletal formations of thin rosettes the film is amorphous, as the accompanying selected area diffraction (SAD) pattern in Fig. 1b shows. (In view of following results, the rosettes are suspected to be incipient spherulites or "crystallization centres", as suggested by Schuster and Gugel [2].) Crystallization started early: in most samples the scale was fully devitrified to spherulitic cristobalite after 1 h at 1400° C. An example is shown in Fig. 2. Only in a few cases were there substantial amounts of amorphous SiO<sub>2</sub> after 1 h and these provided an interesting insight into the devitrification process.

Fig. 3a is a black-and-white reprint of a colour micrograph from a partially crystallized oxide scale. Sharp interference colours appeared as indicated. The round features are spherulites of

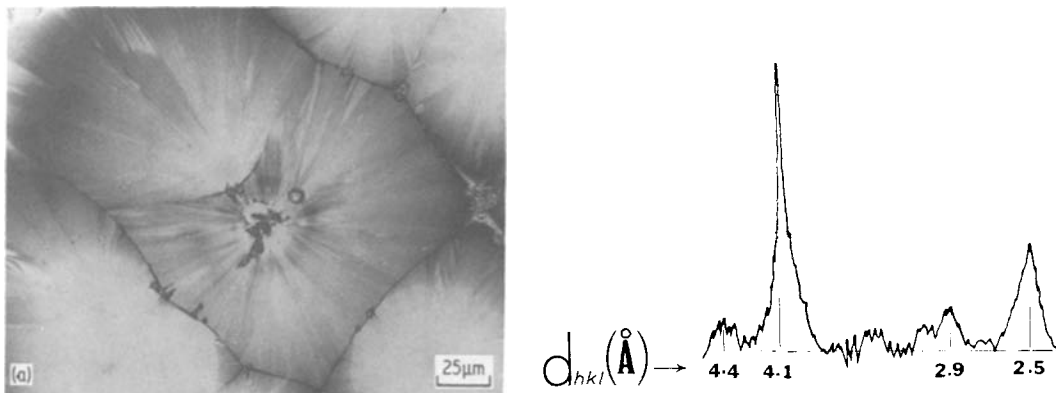


Figure 2 (a) Light micrograph of an oxide scale on technical grade SiC single crystal. The fully devitrified scale is spherulitic. (b) X-ray diffraction identifies the devitrite as cristobalite.

cristobalite, the blue areas between the spherulites are amorphous, as confirmed by the selected area diffraction pattern in Fig. 3b, which was obtained from a triple-point like the ones in Fig. 3a. Because the colours in the micrograph are the complements of the true interference colours the oxide scale is thickest in the blue areas (amorphous pockets). The spherulites themselves exhibit a spectrum of colours. The colour sequence suggests either that the spherulites are dome-shaped or that there is a radial progression in degree of crystallinity and, hence, in refractive index.

The strong interference colours attest to the thinness of the oxide films at this stage. While the spherulites in Figs 2 and 3 are over 100 μm wide, measurements on sectioned samples showed the scales to be much thinner. For instance, after 24 h at 1400° C the scale was only 10 μm thick.

Thus the spherulites are disc-shaped, possibly with domes projecting in the thickening directions. This is to be expected: once nucleated the spherulites would grow fastest laterally, into the amorphous SiO<sub>2</sub>, rather than into the air or the SiC; after mutual impingement lateral growth stops (although amorphous SiO<sub>2</sub> remains at the triple-points) and slow thickening into the air occurs. The suggestion that the cristobalite nucleated in a precursor amorphous film is also very much in line with the well-known spherulitic morphology of silica and silicate devitrites [11–13] and those of amorphous polymeric systems [14].

### 3.2. Spherulitic morphology

The oxide scale in all samples, when crystalline, was always spherulitic. This was the most significant observation. The spherulites grown on the technical grade crystals showed little substructure;

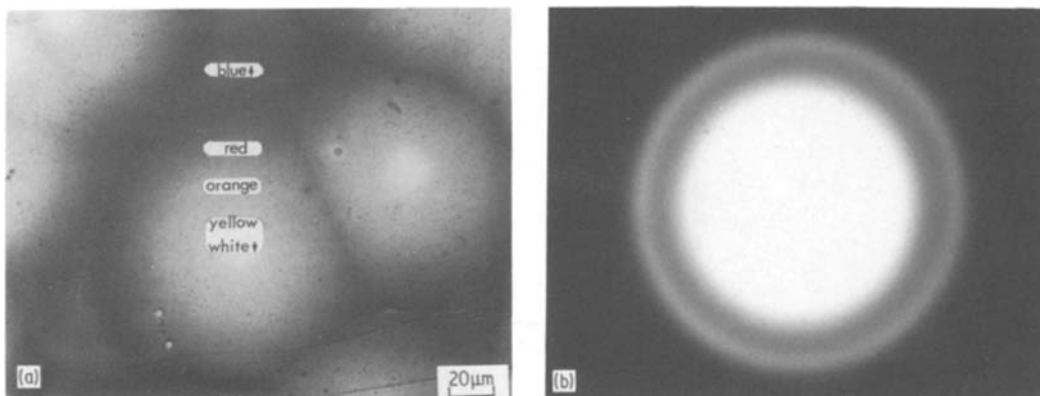
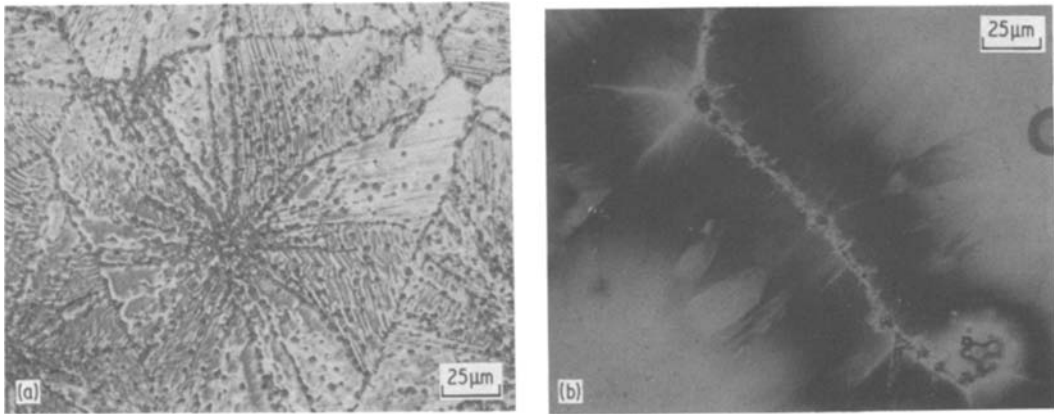


Figure 3 (a) Light micrograph of a partially-devitrified oxide scale on a technical grade sample oxidized for 1 h at 1400° C. Residues of an amorphous oxide occur at triple-points. Observed colours are indicated. (b) SAD pattern from amorphous oxide at a triple-point.



**Figure 4** Light micrographs showing spherulites of cristobalite on SiC single crystals after oxidation for 12 h at 1400° C: (a) semiconductor grade SiC and (b) technical grade SiC.

in contrast, those grown on the semiconductor crystals were usually dendritic within, as Fig. 4 shows. This difference between the two types of specimens is probably due to impurity effects: the semiconductor grade specimens contained minor amounts of dopants or none at all; the commercial grade specimen, on the other hand, probably contained a mix of impurities, the nature and amount of which were not known.

It was pointed out above that spherulitic morphology in silica and silicates is associated with devitrification. It also requires system-specific impurities, as underlined in the theories of Shubnikov [15] and of Keith and Padden [14, 16]. Dendritic growth has similar origins, resulting from thermal destabilization of the crystal growth front, often aided by impurities. Like spherulitic growth, it is not uncommon in the devitrification of amorphous systems [12, 17]. There was no lack of

impurities in some of the specimens studied. Fig. 4 exhibits strings of impurity at the spherulite boundaries. However, the formation of spherulites in the undoped material as well leads to a suspicion that the pertinent impurities came from the atmosphere. The prime candidate is water vapour, whose strong role in the crystallization of vitreous silica and silicates is well known [18, 19] and which is said to accelerate SiC oxidation by promoting devitrification [4, 9].

There was an apparent, inverse correlation between oxidation times and spherulite size: oxidation for longer times seemed to produce spherulites of finer sizes. Compare, for instance, Fig. 5 a and b, showing scales on the technical grade material after 1 and 24 h, respectively; there is about a four-fold decrease in spherulite size. This has been explained in terms of layer-by-layer growth of the spherulites: each successive layer

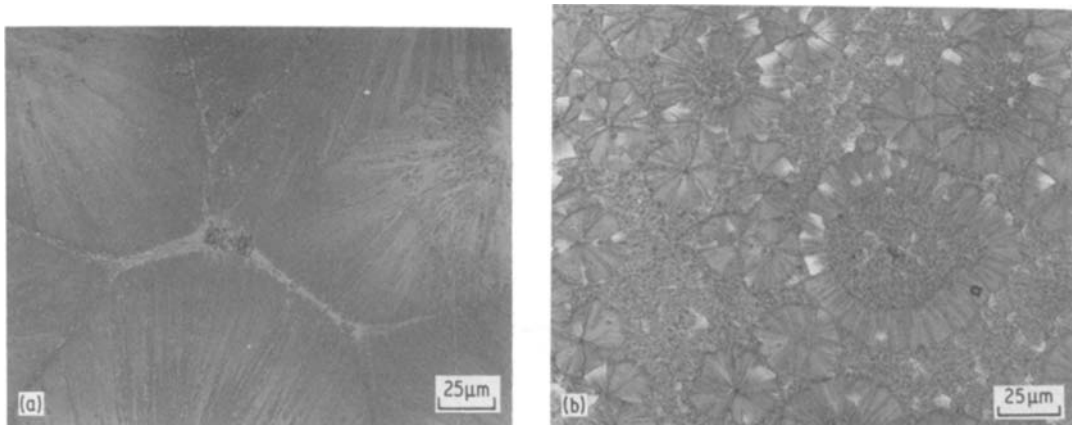


**Figure 5** Light micrographs of technical grade SiC single crystals oxidized at 1400° C for: (a) 1 h (coarse spherulites) and (b) 24 h (finer spherulites).

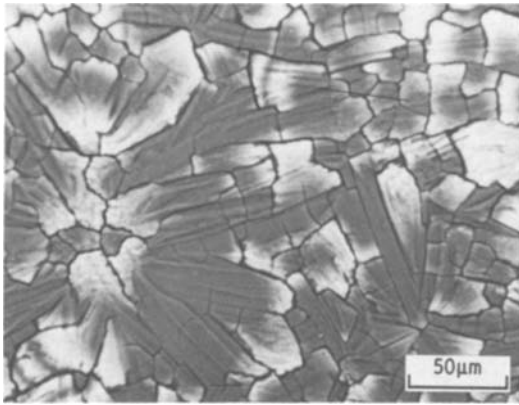


Figure 6 Light micrograph illustrating the loss of spherulitic appearance in the oxide scale with prolonged oxidation (48 h at 1500° C) due to excessive grain growth and thermal etching.

feeds on the less amorphous residue at the triple-points of the preceding layer, thereby developing finer spherulites [8].

With prolonged oxidation at 1400° C or excursion to 1500° C the scale appeared less spherulitic, due to excessive thermal grooving within and around the spherulites, cracking between spherulites and non-uniform grain coarsening. In this situation, shown in Fig. 6 for a

sample oxidized at 1500° C for 48 h, the enhanced boundaries of the individual spherulite subgrains make a stronger impression on the eye than the overall outlines of the spherulitic unit. Similar microstructures have also been observed by other investigators for oxide scales grown on silicon at 1340 to 1390° C [20].

### 3.3. Spherulite crystallography

A characteristic of spherulites is that the radial or tangential direction coincides with the same crystallographic direction in each subgrain [21–23]. This was confirmed by electron diffraction for the spherulites observed here. Fig. 7 shows an electron micrograph of a portion of a spherulite on a sample oxidized for 1 h. Diffraction patterns obtained from the subgrains showed that a  $\langle 111 \rangle^*$  axis was normal or nearly so<sup>†</sup> to the radial direction in each case; thus, the faintly visible, radial striations coincide with the traces of the  $\{111\}$  planes.

Radial alignment of the  $\{111\}$  planes probably satisfies both a kinetic and an energetic need. The habit of geologic cristobalite [11] reveals a preference for growth by extension of the octahedral faces, i.e.  $\{111\}$  planes. The only growth direction possible in a spherically symmetrical system is

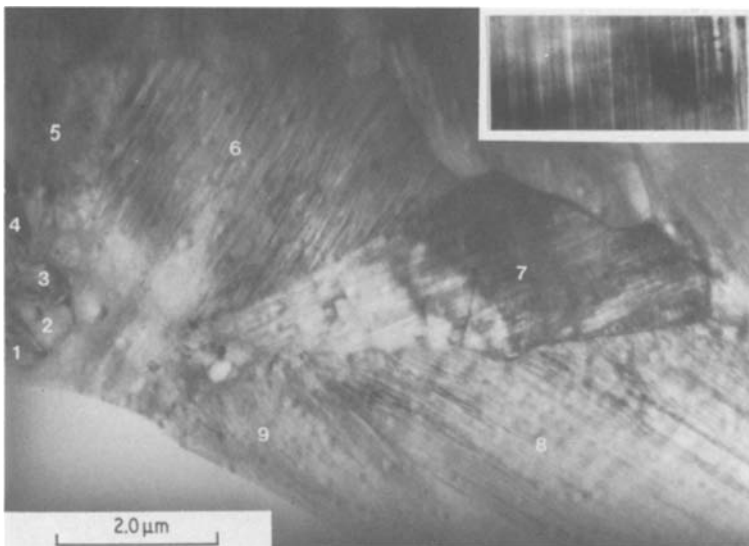


Figure 7 Transmission electron micrographs showing portions of a spherulite: the subgrains are numbered; the faint, radial striations, details inset, are  $\{111\}$  traces.

\*The indices used here refer to the cubic system. It was not determined beyond doubt whether the phase of the cristobalites was  $\beta$  (high) or  $\alpha$  (low) cristobalite. However, this did not present a serious problem:  $\beta$ -cristobalite is cubic, and  $\alpha$ -cristobalite, while it is actually tetragonal, may be considered pseudocubic, as the  $\beta \rightarrow \alpha$  inversion involves a minor dimensional change along only one cube edge.

<sup>†</sup>The limitation is topological: the  $\{111\}$  planes in a subgrain cannot all lie in a radial direction (and remain parallel). As a result, those planes appear inclined to the sub-boundaries in places, but the average orientation remains radial.



Figure 8 Transmission electron micrograph of a cristobalite grain, diffraction pattern inset. The  $\{111\}$  traces are accentuated by electron irradiation damage.

radial; it is therefore not surprising that the preferred growth planes run in that direction. Regarding energies, a spherulite contains a large number of internal boundaries (sub-boundaries misoriented by small angles [14–16]). The energy of each such sub-boundary has to be low to keep the overall system energy low [21, 22]. Because the lowest energy planes are the closest packed ones,  $\{111\}$  in cristobalite, a spherulite can keep its total energy low by aligning those planes parallel\* to the subgrain boundaries, which are themselves radially aligned.

Phase determination in the thicker scales was usually accomplished by X-ray diffraction (Fig. 2b) and sometimes confirmed by selected area electron diffraction analysis (Fig. 7, for instance). Fig. 8 is from a sample oxidized for 24 h at  $1400^\circ\text{C}$ . This spherulite subgrain is imaged near a zone axis identified from the inset diffraction pattern as the  $\langle 110 \rangle$  zone of cristobalite. While the stable phase of silica at the oxidation temperature employed for most samples is tridymite the metastable formation of cristobalite upon crystallization of amorphous silica is very familiar.

However, the occurrence of trace amounts of tridymite in these scales cannot be ruled out. Due to the structural correspondence between cristobalite and tridymite, syntactic growth of both phases is not uncommon. A few subgrains were encountered by TEM in this study whose detailed structure strongly suggested such intergrowth and whose diffraction patterns proved quite difficult

to analyse. Systematic diffraction in such cases was prevented by the rapid rate of radiation damage, leading to a quick loss of crystallinity.

#### 4. Conclusion

It was determined that the oxidation, in air, of variously-doped single crystals of  $\alpha$ -SiC on the basal surfaces yielded scales whose microstructure went from amorphous  $\text{SiO}_2$  to cristobalite as the oxidation progressed. The cristobalite was invariably spherulitic.

#### Acknowledgements

This work was carried out at the Case Western Reserve University, Cleveland, Ohio, and supported by the US AFOSR under contract 75-2789. The author is grateful to T. E. Mitchell and A. H. Heuer for their helpful discussions.

#### References

1. W. F. KNIIPPENBERG, *Philips Res. Rep.* **18** (1963) 161.
2. P. SCHUSTER and E. GUGEL, *Mater. Res. Bull.* **4** (1969) S311.
3. G. ERVIN, Jr, *J. Amer. Ceram. Soc.* **41** (1958) 347.
4. P. J. JORGENSEN, M. E. WADSWORTH and I. B. CUTLER, *ibid.* **42** (1959) 613.
5. J. A. DILLON in "Silicon Carbide" edited by J. R. O'Connor and J. Smittens (Pergamon, New York, 1960) pp. 235–40.
6. R. C. A. HARRIS, *J. Amer. Ceram. Soc.* **58** (1965) 7.
7. E. A. GULBRANSEN, K. F. ANDREW and F. A. BRASSART, *J. Electrochem. Soc.* **113** (1966) 1311.

\*The limitation is topological: the  $\{111\}$  planes in a subgrain cannot all lie in a radial direction (and remain parallel). As a result, those planes appear inclined to the sub-boundaries in places, but the average orientation remains radial.

8. A. H. HEUER, L. U. OGBUJI and T. E. MITCHELL, *J. Amer. Ceram. Soc.* **63** (1980) 354.
9. E. FITZER and R. EBI, in "Silicon Carbide - 1973" edited by R. C. Marshall, J. W. Faust, Jr and C. E. Ryan (University of South Carolina Press, Columbia, SC, 1974) pp. 320-8.
10. J. W. HINZE and W. C. TRIPP, in "Mass Transport Phenomena in Ceramics", edited by A. R. Cooper and A. H. Heuer (Plenum Press, New York, 1975) pp. 409-19.
11. "The System of Mineralogy", Vol. III, edited by C. Frondel (J. Wiley and Sons, New York, 1962).
12. M. H. LEWIS, J. METCALF-JOHANSEN and P. S. BELL, *J. Amer. Ceram. Soc.* **62** (1979) 278.
13. S. W. FREIMAN, G. Y. ONODA, Jr and A. G. PINCUS, *J. Amer. Ceram. Soc.* **55** (1972) 354.
14. H. D. KEITH and F. J. PADDEN, Jr, *JAP* **34** (1963) 2409.
15. A. V. SHUBNIKOV, *Sov. Phys. Crystallog.* **2** (1959) 578.
16. H. D. KEITH and F. J. PADDEN, Jr, *J. Appl. Phys.* **35** (1964) 1270.
17. R. H. REDWINE and M. A. CONRAD, in "Ceramic Microstructures" edited by R. M. Fulrath and J. A. Pask (J. Wiley and Sons, New York, 1968) pp. 900-22.
18. F. E. WAGSTAFF and K. J. RICHARDS, *J. Amer. Ceram. Soc.* **59** (1966) 118.
19. F. W. AINGER, *J. Mater. Sci.* **1** (1966) 1
20. W. C. TRIPP and J. W. HINZE, "Internal Structure and Physical Properties of Ceramics at High Temperatures", Aerospace Research Laboratories Final Report ARL TR 75-1030, June 1975.
21. B. LUX, *American Foundrymen's Society Cast Met. Res. J.* **8** (1972) 25.
22. W. BOLLMAN and B. LUX, Proceedings of the International Conference on the Metallography of Cast Iron, edited by B. Lux, I. Minkoff and F. Mollard (Georgi Publishing Company, Saphorin, Switzerland, 1974) pp. 461-71.
23. C. E. MILLER, *J. Cryst. Growth* **42** (1977) 357.

Received 27 October 1980 and accepted 26 March 1981.